Available online at www.sciencedirect.com

ScienceDirect

Procedia Engineering 4 (2010) 99–105

Procedia Engineering

www.elsevier.com/locate/procedia

ISAB-2010

Evaluation of wave force acting on Submerged Floating Tunnels

Hiroshi Kunisu*

T.K. Gotanda Bldg., 8-3-6 Nishi Gotanda, Shinagawa-Ward Tokyo 141-0031 Japan

Received 29 July 2010; revised 2 August 2010; accepted 3 August 2010

Abstract

The purpose of this study is to investigate the wave force characteristics acting on the Submerged Floating Tunnel (SFT). When the wave force acting on a large size structure is estimated such as ships and floating platforms, the diffraction theory based on the velocity potential is often used because the inertial force is dominant for the wave force evaluation. If the structural size is rather small and the drag term cannot be neglected, on the other hand, the empirical equation known as Morison's equation is widely used. SFT is a completely submerged structure and the size of that may differ from a small one for pipeline to a large one for highway or railroad system. It is obvious that an appropriate evaluation of wave force is essential for predicting the dynamic response due to wave. In this study, the wave force was evaluated based on the diffraction theory by Boundary Element Method first, and the effects of the size and the shape of SFT on the wave force are discussed. Second, the Morison's equation which can estimate both drag and inertial forces was applied to evaluate the role of drag force. Those results were compared with experimental results and the findings through those studies are introduced.

Keywords: wave force, submerged floating tunnel; boundary element method; Morson's equation; K.C. number; drag force; inertia force

1. Introduction

Evaluation of wave force acting on structure has been investigated for many years. For a floating object such as ship and barges, Finite Strip Method (FSM) and Boundary Element Method (BEM) have been applied for solving the Laplace equation based on the velocity potential. In the case of relatively small structures like a structural member of truss, the Morison's equation has been widely used. As it is broadly known, the velocity potential is applicable when the inertia force with diffraction is predominant to the drag force. On the other hand, the Morison's equation considers both inertia and drag terms although it is an empirical equation with simplified coefficients for drag and inertia forces and they are depending on Reynold's number, Re, and Kuelegan-Carpenter number, K.C. [1]. In the case of Submerged Floating Tunnel (SFT), the structure itself is completely submerged and the size of that may cover wide range in its diameter and in the length. In addition, it is very important to estimate the fluid force appropriately due to wave because it significantly affects on the dynamic response of SFT.

Experimental studies on large size structure, for example, have been carried out for developing strait crossing structures [2-4]. In Japan, investigation of submerged floating tunnel was started in 1990. Numerical analysis of wave force and dynamic response of the submerged floating tunnels were studied [5]. This paper introduces the characteristics of wave force acting on Submerged Floating Tunnel (SFT) with analytical and experimental results.

2. Estimation method of wave force

2.1. Boundary element method for diffraction theory based on the velocity potential

Assuming that the fluid is not compressive without rotation, the governing equation can be expressed by the following equation.

* Corresponding author. Tel.: +81-3-5434-8185; fax: +81-3-5434-5393.
E-mail address: Hiroshi_Kunisu@jportc.co.jp

doi:10.1016/j.proeng.2010.08.012

$$\nabla^2\varphi = \frac{\partial^2\varphi}{\partial x^2} + \frac{\partial^2\varphi}{\partial z^2} = q \tag{1}$$

$\varphi = \varphi_i + \varphi_D$: velocity potential, φ_i : velocity potential of incident waves, φ_D : velocity potential of diffraction waves, q: volume flux density.

We assume that a rigid body is floating in the fluid as shown in Fig. 1 with the boundary conditions given by the following equations.

$$\phi = \frac{gH_0}{\omega}\left\{e^{ikl} + K_r e^{-ikl}\right\}\frac{\cosh k(z+h)}{\cosh kh} \quad \textit{(on a – b)} \tag{2}$$

$$\frac{\partial\phi}{\partial n} = -ik\frac{gH_0}{\omega}\left\{-e^{ikl} + K_r e^{-ikl}\right\}\frac{\cosh k(z+h)}{\cosh kh} \quad \textit{(on a – b)} \tag{3}$$

$$\frac{\partial\phi}{\partial z} - \frac{\omega^2}{g}\phi = 0 \quad (\text{on } S_F) \tag{4}$$

$$\frac{\partial\phi}{\partial z} = 0 \quad (\text{on } S_B) \tag{5}$$

$$\frac{\partial\varphi}{\partial n} = v_n \quad (\text{on } S_V) \tag{6}$$

$$\phi = \frac{gH_0}{\omega}K_t e^{-ikl}\frac{\cosh k(z+h)}{\cosh kh} \quad \textit{(on c – d)} \tag{7}$$

$$\frac{\partial\phi}{\partial n} = -ik\frac{gH_0}{\omega}K_t e^{-ikl}\frac{\cosh k(z+h)}{\cosh kh} \quad \textit{(on c – d)} \tag{8}$$

ω: phase velocity, k: wave number, H_0: height of incident wave, n: direction normal, K_r: reflection ratio, K_t: passing ratio, v_n : velocity of fluid in normal direction.

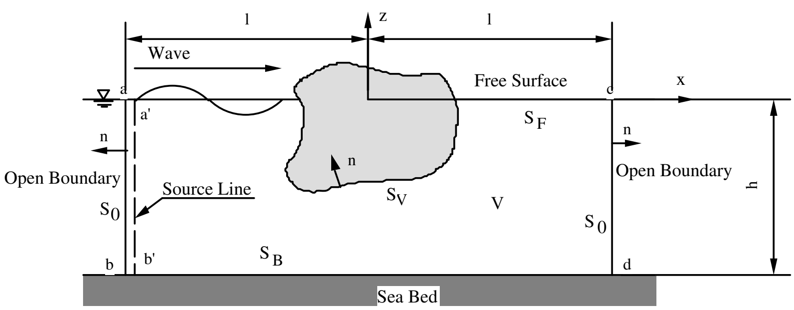

Fig. 1. Modelling of fluid and structure with boundary conditions

After applying Green's function, the descretized equation for BEM is derived as follows [7-8].

$$\frac{1}{2}\varphi_i + \int_{\Gamma1+\Gamma2}\frac{\partial v}{\partial n}\varphi_D d\Gamma + \int_{\Gamma3}\left(\frac{\partial v}{\partial n} - ikv\right)\varphi_D d\Gamma + \int_{\Gamma4}\left(\frac{\partial v}{\partial n} - \frac{\sigma^2}{g}\right)\varphi_D d\Gamma = \int_{\Gamma1} v\frac{\partial\varphi_D}{\partial n}d\Gamma \tag{9}$$

Γ : boundary condition (1: body surface, 2: sea bed, 3: side flux, 4: free surface).

The fluid pressure and the resultant forces due to pressure in horizontal and vertical directions are given by the following equations.

$$p(x, y) = -\rho \frac{\partial \phi_D}{\partial t} \tag{10}$$

$$F_x = -\oint_{\Gamma_1} p(x, y) n_x dS \tag{11}$$

$$F_y = \oint_{\Gamma_1} p(x, y) n_y dS \tag{12}$$

$p(x, y)$: wave pressure around the SFT, F_x, F_y : wave force.

2.2. Morison's equation

The Morison's equation is widely used to estimate fluid force acting on a submerged object. If the velocity and the acceleration of fluid are given at the representing position of the object, it is easy to evaluate wave force including drag and inertia terms based on an empirical equation [9]. The equation includes two coefficients such as C_d and C_M corresponding to the drag and the inertia force respectively. Those coefficients can be fixed based on the shape of the object. The Morison's equation is as shown in Eq. (13).

$$F = \frac{1}{2} \rho A C_d u |u| + \rho V C_M \frac{du}{dt} \tag{13}$$

F: wave force, C_d : drag force coefficient, C_M : inertia force coefficient, u : velocity of fluid , A: area of SFT, V: volume of SFT.

3. Comparison of estimated wave forces with experimental results

Considering the strength of SFT to other conventional crossing structures such as bridge and immersed tunnel, SFT is applicable for large water depth. Then, it is assumed that the water depth for wave force estimation is as deep as 100 m. Fig. 2 illustrates the standard calculation conditions and the effects of the diameter, the installed depth, and the exterior shape of SFT on the wave force are investigated. All the wave forces are normalized by the following equation with the specific weight of the fluid and the wave height.

$$f = \frac{F}{w_0 \cdot \frac{H}{2}} \tag{14}$$

f: non-dimensional wave force, *H*: wave height, *T*: wave period and *D*: diameter of SFT, $w_0 = \rho g$: unit weight of fluid, g: gravity acceleration.

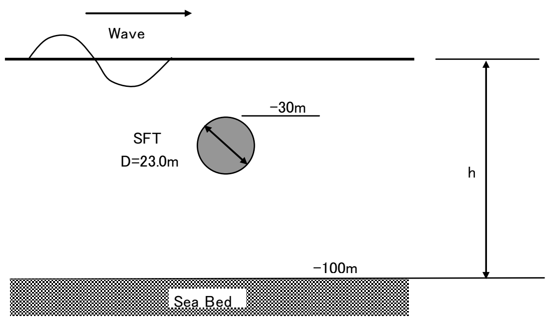

Fig. 2. Standard calculation condition for wave force

3.1. Evaluation by BEM

The vertical and horizontal wave forces acting on the SFT are estimated as shown in Fig. 3. The vertical axis stands for the normalized wave force and the horizontal axis gives the wave number. The observed data in experiment are also plotted in the same figure. From this figure, it is understood that the numerical evaluation almost coincide with the experimental data. The wave force is strongly depending on the wave number and its peak value is recorded at around 0.2 in the wave number.

Second, the effect of the installation depth of SFT on the wave force is investigated. It is assumed that the diameter of the tunnel is fixed at 23 m and the water depth is 100m. The clearance above the tunnel is described as crown depth and the wave forces were estimated for different crown depths of 30m, 50m and 70m. The results are shown in Fig. 4. As seen in this figure, the peak value in wave force decreases with the increase in the crown depth and those maximum values are recorded at smaller wave numbers than that for the standard condition of 30 m in the crown depth.

The effect of the shape of SFT on the wave force is another interesting issue for designers. The wave force is estimated by the BEM when the elliptical shape was adopted for the exterior shape of SFT instead of the round shape. In this calculation, the height of the tunnel was fixed as 23 m and the width was set at 35 m. Fig. 5 shows the results of calculation. Since the mass of water displaced by the tunnel is larger than that by round-shape tunnel, the wave force itself becomes larger, of course. However, the wave forces in both directions sharply increase with the wave numbers and it can be understood that the wave force is depending on the wave number more sensitively. In addition, rotational moment is caused due to wave force. Therefore, round-shape SFT is preferable than elliptical one and the designer should be careful for the increase in wave force when round-shape SFT cannot be adopted.

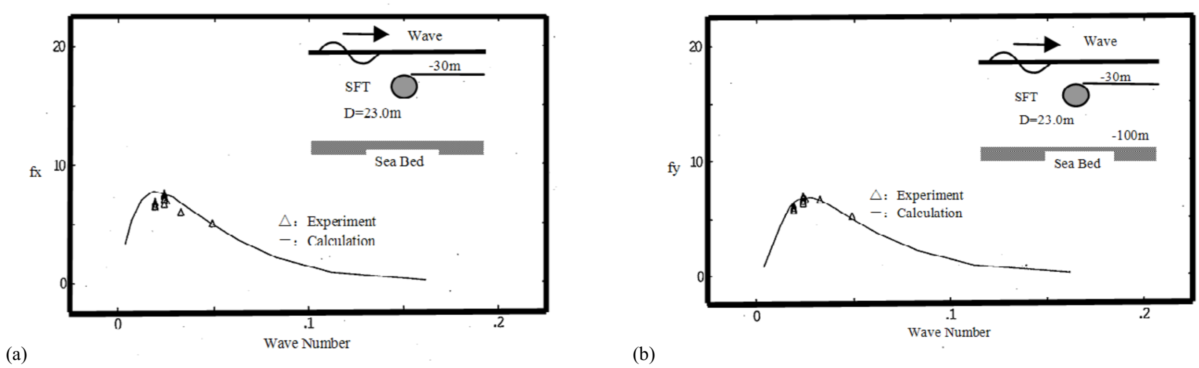

Fig. 3. Comparison of calculated wave force with experimental results: (a) Transverse direction; (b) Vertical direction

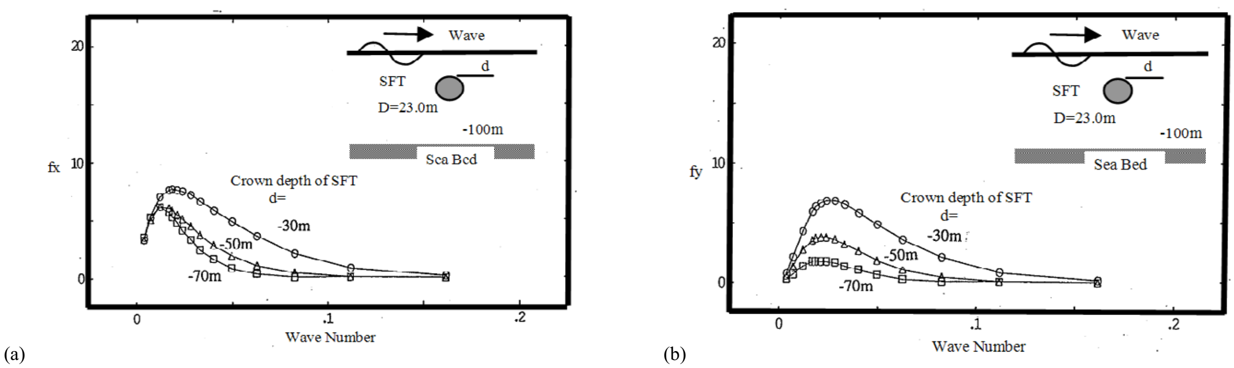

Fig. 4. Characteristics of wave force in different crown depth of tunnel evaluated by BEM: (a) Transverse direction; (b) Vertical direction

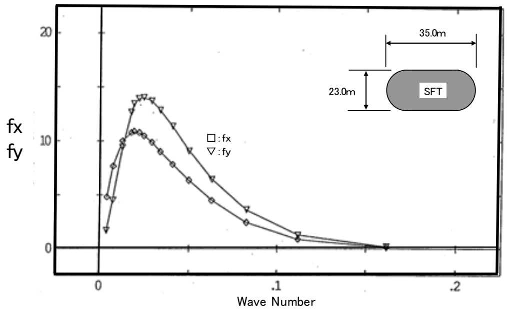

Fig. 5. Wave force characteristics acting on SFT with elliptical shape

3.2. Evaluation by the Morison's equation

The first figure named as (a) in Fig. 6 shows the time series of drag and inertia forces acting on the SFT calculated by the Morison's equation. In order to evaluate the effect of drag term on the whole fluid force, the time history of the drag force is also shown in the same figure. It can be seen that the inertia force is more dominant than the drag force in this case because the diameter of the tunnel is large enough to neglect the drag force. Although the difference in phase delay of peak amplitudes between the drag force and the inertia force is 90 degrees, the maximum amplitude of fluid force is recorded at the almost same time with that of inertia force.

In (b) and (c) of Fig. 6, the relationships between the wave force and the wave period are illustrated. The drag force shown in (b) increases linearly with increase in the wave period at the beginning and it converges finally. On the other hand, the inertia force has a peak value at some period as same as the results by BEM.

$$K.C. = \frac{u \cdot T}{D} \tag{15}$$

u: velocity of fluid, T: wave period, D: diameter of SFT.

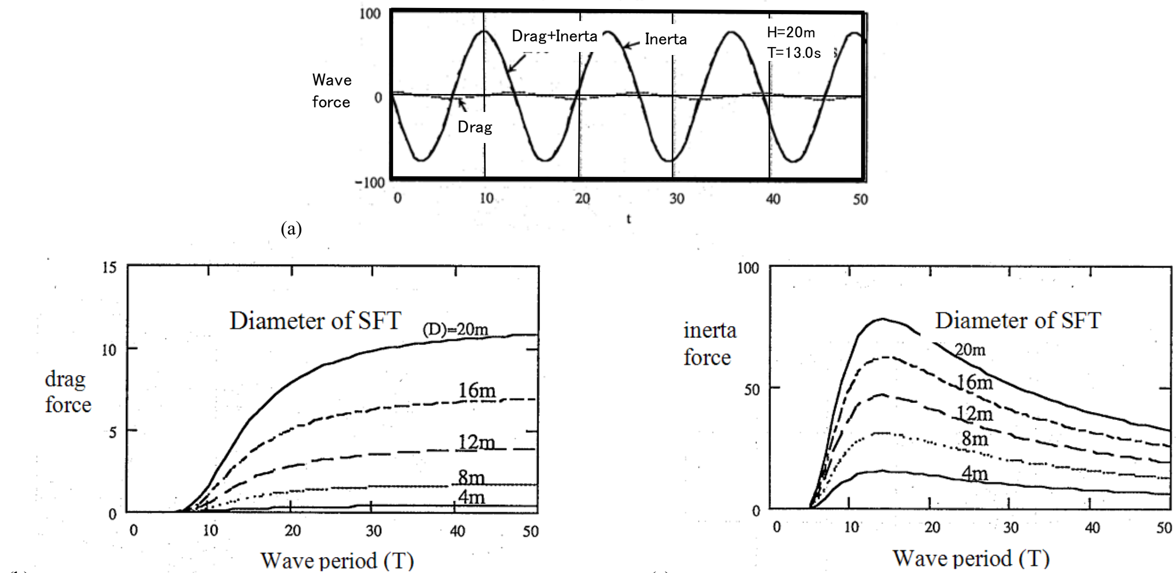

Fig. 6. Effect of drag force and inertia force acting on SFT: (a) Time series of wave force acting on SFT; (b) Drag force; (c) Inertia force

3.3. Comparison of estimation method with experimental data

As a result of the experiment, drag force and inertia force coefficients were obtained as shown in Fig.7. Those figures show the relation between the coefficient of drag or inertia force and the Keulegan-Carpenter Number. For the calculation of round-shaped object, the value of 2.0 is recommended as an added mass coefficient and it is confirmed by the experiment although the coefficient of 2.0 may overestimate the inertia force for a large Keulegan-Carpenter number (K.C. number). On the other hand, the value of the drag force coefficient is scattering when the K.C. number is small. This might be caused by noise during the experiment (Kunisu 1994) since the value of drag force coefficient is so small to observe accurately. Fig. 8 shows the results of estimated wave force by BEM based on the potential theory（Bird 1982）with the results by the Morison's equation (C_d=1.0, C_m=2.0）and experimental results. Estimated wave forces by BEM and the Morison's equation show good agreements with the experimental results.

The fluid force due to wave has a close relation with K.C. number (Kuelegan-Carpenter 1958). From the calculation results, Fig. 9 shows to judge the predominant component in fluid force. From this figure, the inertia force is predominant when the K.C. number is less than 15.

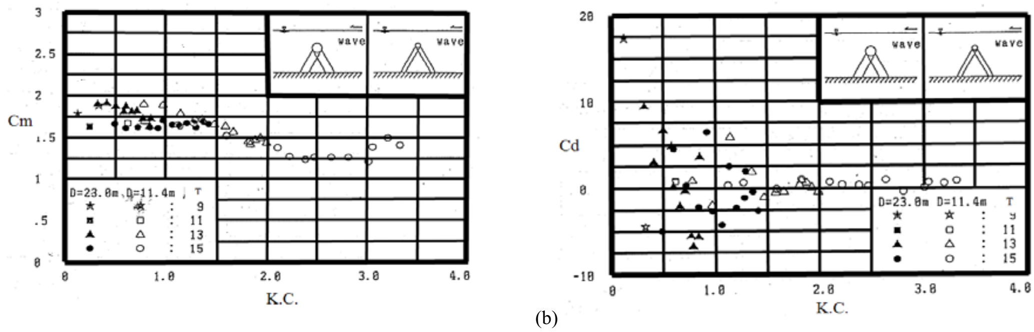

(a) (b)

Fig. 7. Experimental results of drag force and inertia force coefficient of SFT: (a) Inertia force coefficient of SFT; (b) Drag force coefficient

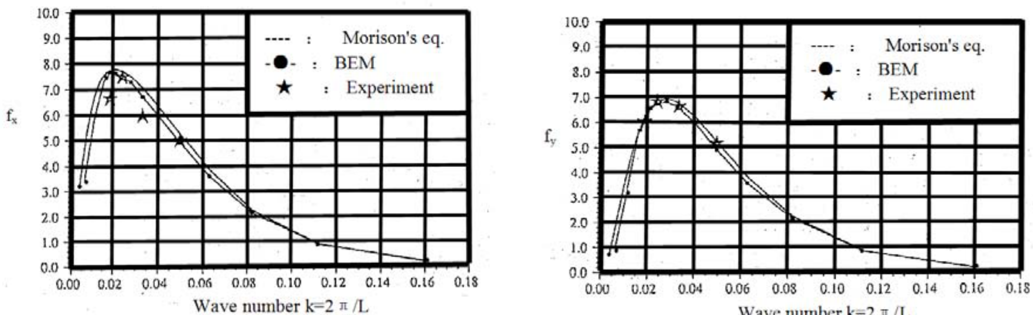

(a) (b)

Fig. 8. Estimation wave force using of Morison's equation: (a) Wave force of transverse direction; (b) Wave force of vertical direction

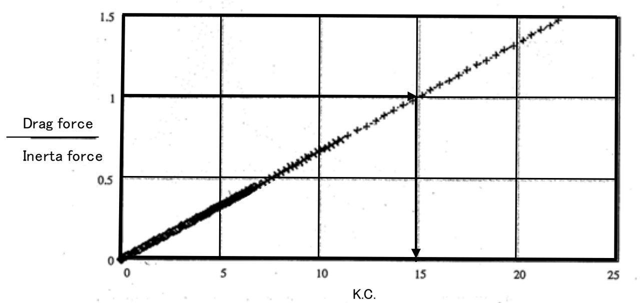

Fig. 9. Wave force regime

4. Conclusion

The analytical and experimental study on fluid force acting on SFT is concluded as follows.

- As a result of this study, it is shown that the wave force acting on the submerged floating tunnel can be calculated accurately by applying both Morrison's equation and Boundary Element Method.
- It is also recognized that the drag force and the inertia force simultaneously work on the submerged floating tunnel.
- In the case of SFT with large diameter, the inertia force is dominant when the K.C. number is less than 15.

Acknowledgements

This study was carried out under the commission of the Society of submerged Floating Tunnel Technology Research in Hokkaido, which consisted of Hokkaido University, the Bureau of Hokkaido development and numerous industries. My special appreciation goes to the members of the subcommittee for Fluid Force Research for their great support on my work.

References

[1] Sarpkaya. Wave forces on cylindrical piles on the sea. *Ocean Engineering Science* 1982; 9, Part A.

[2] Ostlid H. Development of the Norwegian tube bridges. *The 2nd Symposium on Strait Crossings*, Trondheim, Norway; 1990, p.399–400.

[3] Dahle LA, Reed K, Aarsnes JV. Considerration for desing of downward non-anchred submerged tubes. *The 2nd Symposium on Strait Crossings,* Trondheim, Norway; 1990, p.401–408.

[4] Tavit P, et al. Downward arched immersed tubes for road traffic spanning between shores of deep fijords. *International Symposium on Strate Crossings,* Oroceedings Stvanger, Norway; 1986.

[5] Kunisu H, Mizuno S, Mizuno Y, Yamasita T, Saeki H. Numerical analysis of wave force and dynamic response to the submerged floating tunnels. *Strait crossing* 1994.

[6] Bureau of Standards, 60(5): 423-440.

[7] Brancaleoni F, Castellani A, D'Asdia P. The response of submerged tunnels to their environment. *Engng Struct* 1989; 11: 47–56.

[8] AHK Bird, R Shepherd. Wave interaction with large submerged structures. ASCE, WW2, 1982; p.146-162.

[9] Morison JS, O'Brien MP, Johnson JW , Schaaf SA. The force exerted by surface wave on piles. *Petol. Trans., AIME* 1950; 189: 149–154.

[10] Kunisu H, Mizuno Y, Saeki H. Wave force characteristics acting on the submerged floating tunnel. *International Workshop on Floating Structures in Coastal Zone* 1994.

[11] Bird HWK, Shepherd R. Wave interaction with large submerged structures. ASCE, ww2, 1982; p.146-162.

[12] Keulegan GH, Capenter LH. Force on cylinders and plates in an oscillating fluid. *J.Res.* Nat 1958.